Biomedical Optics EXPRESS

Nanosecond laser pulse stimulation of the inner ear—a wavelength study

Michael Schultz,[1,2,*] Peter Baumhoff,[1] Hannes Maier,[1] Ingo U. Teudt,[1] Alexander Krüger,[2] Thomas Lenarz,[1] and Andrej Kral[1]

[1]*Institute of Audioneurotechnology (VIANNA) & Dept. of Experimental Otology, ENT-Clinics, Medical University Hannover, Feodor-Lynen-Straße 35, 30625 Hannover, Germany*
[2]*Laser Zentrum Hannover e.V., Hollerithallee 8, 30419 Hannover, Germany*
*m.schultz@lzh.de

Abstract: Optical stimulation of the inner ear, the cochlea, is discussed as a possible alternative to conventional cochlear implants with the hypothetical improvement of dynamic range and frequency resolution. In this study nanosecond-pulsed optical stimulation of the hearing and non-hearing inner ear is investigated *in vivo* over a wide range of optical wavelengths and at different beam delivery locations. Seven anaesthetized guinea pigs were optically stimulated before and after neomycin induced destruction of hair cells. An optical parametric oscillator was tuned to different wavelengths (420 nm–2150 nm, ultraviolet to near-infrared) and delivered 3–5 ns long pulses with 6 µJ pulse energy via a multimode optical fiber located either extracochlearly in front of the intact round window membrane or intracochlearly within the scala tympani. Cochlear responses were measured using registration of compound action potentials (CAPs). With intact hair cells CAP similar to acoustic stimulation were measured at both locations, while the neomycin treated cochleae did not show any response in any case. The CAP amplitudes of the functional cochleae showed a positive correlation to the absorption coefficient of hemoglobin and also to moderate water absorption. A negative correlation of CAP amplitude with a water absorption coefficient greater than 5.5 cm^{-1} indicates additional phenomena. We conclude that in our stimulation paradigm with ns-pulses the most dominant stimulation effect is of optoacoustic nature and relates to functional hair cells.

OCIS codes: (110.5125) Photoacoustics; (170.4940) Otolaryngology; (170.1065) Acousto-optics; (330.5380) Physiology; (140.3600) Lasers, tunable; (010.7340) Water; (010.1030) Absorption.

References and links

1. M. F. Dorman and B. S. Wilson, "The design and function of cochlear implants," Am. Sci. **92**, 436–445 (2004).
2. A. Kral and G. M. O'Donoghue, "Profound deafness in childhood," N. Engl. J. Med. **363**(15), 1438–1450 (2010).
3. A. Kral, R. Hartmann, D. Mortazavi, and R. Klinke, "Spatial resolution of cochlear implants: the electrical field and excitation of auditory afferents," Hearing Res. **121**(1-2), 11–28 (1998).
4. A. D. Izzo, J. T. Walsh, Jr., J. Pathria, E. Suh, C.-P. Richter, D. S. Whitlon, and E. D. Jansen, "Selectivity of optical stimulation in the auditory system," Proc. SPIE **6078**, 60781P (2006).
5. A. D. Izzo, C.-P. Richter, E. D. Jansen, and J. T. Walsh, Jr., "Laser stimulation of the auditory nerve," Lasers Surg. Med. **38**(8), 745–753 (2006).
6. M. A. Gimeno, C. M. Robets, and J. L. Webb, "Acceleration of rate of the early chick embryo heart by visible light," Nature **214**(5092), 1014–1016 (1967).
7. M. W. Jenkins, A. R. Duke, S. Gu, Y. Doughman, H. J. Chiel, H. Fujioka, M. Watanabe, E. D. Jansen, and A. M. Rollins, "Optical pacing of the embryonic heart," Nat. Photonics **4**(9), 623–626 (2010).
8. M. G. Shapiro, K. Homma, S. Villarreal, C.-P. Richter, and F. Bezanilla, "Infrared light excites cells by changing their electrical capacitance," Nat Commun. **3**, 736 (2012).
9. I. U. Teudt, H. Maier, C.-P. Richter, and A. Kral, "Acoustic events and "optophonic" cochlear responses induced by pulsed near-infrared laser," IEEE Trans. Biomed. Eng. **58**(6), 1648–1655 (2011).

#174557 - $15.00 USD Received 17 Aug 2012; revised 13 Nov 2012; accepted 23 Nov 2012; pub. 28 Nov 2012

10. G. I. Wenzel, S. Balster, K. Zhang, H. H. Lim, U. Reich, O. Massow, H. Lubatschowski, W. Ertmer, T. Lenarz, and G. Reuter, "Green laser light activates the inner ear," J. Biomed. Opt. **14**(4), 044007 (2009).
11. K. Y. Zhang, G. I. Wenzel, S. Balster, H. H. Lim, H. Lubatschowski, T. Lenarz, W. Ertmer, and G. Reuter, "Optoacoustic induced vibrations within the inner ear," Opt. Express **17**(25), 23037–23043 (2009), http://www.opticsinfobase.org/abstract.cfm?URI=oe-17-25-23037.
12. A. Vogel and V. Venugopalan, "Mechanisms of pulsed laser ablation of biological tissues," Chem. Rev. **103**(2), 577–644 (2003).
13. C.-P. Richter, A. I. Matic, J. D. Wells, E. D. Jansen, and J. T. Walsh, Jr., "Neural stimulation with optical radiation," Laser Photonics Rev. **5**(1), 68–80 (2011).
14. I. Sendowski, A. Braillon-Cros, and C. Delaunay, "CAP amplitude after impulse noise exposure in guinea pigs," Eur. Arch. Otorhinolaryngol. **261**(2), 77–81 (2004).
15. G. M. Hale and M. R. Querry, "Optical constants of water in the 200-nm to 200-µm wavelength region," Appl. Opt. **12**(3), 555–563 (1973).
16. K. F. Palmer and D. Williams, "Optical properties of water in the near infrared," J. Opt. Soc. Am. **64**(8), 1107–1110 (1974).
17. S. Prahl, "Optical absorption of hemoglobin" (1998), tabulated molar extinction coefficient for hemoglobin in water using data from W. B. Gratzer, Medical Research Council Labs, Holly Hill, London, UK and N. Kollias, Wellman Laboratories, Harvard Medical School, Boston, MA, USA, at http://omlc.ogi.edu/spectra/hemoglobin/index.html.
18. The correlation between CAP amplitude and both absorption coefficients is a consequence of a mutual negative correlation of the absorption coefficients ($r_{HbO2vsWater}^2 = 0.57$, $p < 0.001$).
19. J. J. Eggermont, "Analysis of compound action potential responses to tone bursts in the human and guinea pig cochlea," J. Acoust. Soc. Am. **60**(5), 1132–1139 (1976).
20. C.-P. Richter and A. I. Matic, "Chapter 6: Optical stimulation of the auditory nerve," in *Auditory Prostheses: New Horizons*, F.-G. Zeng, A. N. Popper, and R. R. Fay, eds. (Springer, 2011), pp. 135–156.
21. C.-P. Richter, R. Bayon, A. D. Izzo, M. Otting, E. Suh, S. Goyal, J. Hotaling, and J. T. Walsh, Jr., "Optical stimulation of auditory neurons: effects of acute and chronic deafening," Hearing Res. **242**(1-2), 42–51 (2008).
22. E. F. Carome, N. A. Clark, and C. E. Moeller, "Generation of acoustic signals in liquids by ruby laser induced thermal stress transients," Appl. Phys. Lett. **4**(6), 95–97 (1964).
23. A. G. Bell, *Upon the Production of Sound by Radiant Energy* (Gibson Brothers, Washington, D.C., 1881), pp. 1–45
24. K. P. Köstli, M. Frenz, H. P. Weber, G. Paltauf, and H. Schmidt-Kloiber, "Optoacoustic infrared spectroscopy of soft tissue," J. Appl. Phys. **88**(3), 1632–1637 (2000).
25. S. M. Rajguru, C.-P. Richter, A. I. Matic, G. R. Holstein, S. M. Highstein, G. M. Dittami, and R. D. Rabbitt, "Infrared photostimulation of the crista ampullaris," J. Physiol. **589**(6), 1283–1294 (2011).
26. R. L. Fork, "Laser stimulation of nerve cells in Aplysia," Science **171**(3974), 907–908 (1971).
27. I. U. Teudt, A. E. Nevel, A. D. Izzo, J. T. Walsh, Jr., and C.-P. Richter, "Optical stimulation of the facial nerve: A new monitoring technique?" Laryngoscope **117**(9), 1641–1647 (2007).
28. J. Wells, C. Kao, K. Mariappan, J. Albea, E. D. Jansen, P. Konrad, and A. Mahadevan-Jansen, "Optical stimulation of neural tissue in vivo," Opt. Lett. **30**(5), 504–506 (2005).
29. F. J. Julian and D. E. Goldman, "The effects of mechanical stimulation on some electrical properties of axons," J. Gen. Physiol. **46**(2), 297–313 (1962).
30. F. Sachs, "Stretch-activated ion channels: What are they?" Physiology (Bethesda) **25**(1), 50–56 (2010).
31. M. A. Ruggero and A. N. Temchin, "Similarity of traveling-wave delays in the hearing organs of humans and other tetrapods," J. Assoc. Res. Otolaryngol. **8**(2), 153–166 (2007).
32. P. Magnan, P. Avan, A. Dancer, J. Smurzynski, and R. Probst, "Reverse middle-ear transfer function in the guinea pig measured with cubic difference tones," Hearing Res. **107**(1-2), 41–45 (1997).
33. C. A. Miller, P. J. Abbas, J. T. Rubinstein, B. K. Robinson, A. J. Matsuoka, and G. Woodworth, "Electrically evoked compound action potentials of guinea pig and cat: responses to monopolar, monophasic stimulation," Hearing Res. **119**(1-2), 142–154 (1998).
34. A. D. Izzo, J. T. Walsh, Jr., E. D. Jansen, M. Bendett, J. Webb, H. Ralph, and C.-P. Richter, "Optical parameter variability in laser nerve stimulation: a study of pulse duration, repetition rate, and wavelength," IEEE Trans. Biomed. Eng. **54**(6), 1108–1114 (2007).
35. E. D. Jansen, T. G. van Leeuwen, M. Motamedi, C. Borst, and A. J. Welch, "Temperature dependence of the absorption coefficient of water for midinfrared laser radiation," Lasers Surg. Med. **14**(3), 258–268 (1994).
36. G. Paltauf, H. Schmidt-Kloiber, and M. Frenz, "Photoacoustic waves excited in liquids by fiber-transmitted laser pulses," J. Acoust. Soc. Am. **104**(2), 890–897 (1998).

1. Introduction

The high incidence of hearing loss and the success of neuroprosthetic therapy of hearing loss using implants in the inner ear (cochlea) have resulted in an increasing interest in artificial stimulation of the cochlea [1,2]. Cochlear implants replace a non-functional inner ear by an electrode array that stimulates the auditory nerve. Recently, laser stimulation of the cochlea

#174557 - $15.00 USD Received 17 Aug 2012; revised 13 Nov 2012; accepted 23 Nov 2012; pub. 28 Nov 2012

has attracted attention owing to the high spatial precision of this stimulation, particularly if compared with electrical fields ([3] vs. [4]). Pulsed near-infrared lasers are among the means suggested for increasing the number of independent channels used in cochlear stimulation [5]. Previous studies reported reactions to sunlight and laser light in excitable tissue, one example being the optical pacing of the heart [6,7]. The mechanisms, however, remain obscure [8], and the results of optical stimulation of the cochlea are still ambiguous. Initial findings with µs pulses at a wavelength of ≈1850 nm reported direct neuronal stimulation [5], but a recent study with the same laser system pointed to acoustic phenomena responsible for cochlear excitation [9]. The laser-evoked sounds were well audible (≈60 dB sound pressure level (SPL)) and could be acoustically masked. Two unspecific mechanisms of excitation were recently suggested: either modulation of membrane capacitance by heat due to absorption of the laser light in water [8] or hair cell stimulation via optoacoustic effects [9–11].

It remains largely unknown how cochlear responses depend on physical characteristics of the laser light. Generally, laser tissue interaction can be classified into no confinement, thermal confinement, and stress confinement depending on laser pulse parameters [12]. The key laser parameters determining the type of laser tissue interaction are wavelength, pulse duration, radiant exposure, pulse energy, peak power, and repetition rate. The exploration of the corresponding parameter space requires more than one laser device. So far, the influence of wavelength has not been investigated independently; rather, different laser devices with different laser parameters have been used ([5,9,10,13] and the references therein). Consequently, it is impossible to determine the influence of a single parameter, such as wavelength. In our study, one tunable laser system with constant pulse duration was used. The wavelength was chosen between 420 nm and 2150 nm. Determining the wavelength dependency of cochlear responses allows conclusions on candidate stimulation mechanisms.

Present data show a sensitivity of the cochlear response to wavelength of the laser at constant pulse duration and energy. Several wavelength regions have been identified that correlate with water or hemoglobin absorption and therefore indicate different interaction sites. Finally, independent of the type of interactions, the present data also demonstrate that the latency of the response is a linear function of its amplitude. The absence of responses in completely deaf animals demonstrates the dependency of cochlear excitation on hair cells using the present laser pulse parameters.

2. Materials and methods

2.1. Guinea pig surgery and monitoring of cochlear function

The experimental design was approved by German state authorities. Animal handling and preparation were in accordance with the German and European Union guidelines for animal research and were approved by German state authorities.

Seven adult Dunkin-Hartley guinea pigs (Harlan, 1–4 months) of either sex were anesthetized by intramuscular injection of 50 mg/kg 2% ketamine solution (CP Pharma, Burgdorf, Germany) and 10 mg/kg 10% xylazine solution (WDT, Garbsen, Germany) volume-adjusted to the animals' body weight. The initial anesthesia dose contained 0.1mg/kg atropine sulfate (B. Braun, Melsungen, Germany) to prevent mucous obstruction of airways during surgery. Anesthesia level was assessed by continuous monitoring of heart rate (using ECG) and capnometry. Additionally, the paw-pinch withdrawal reflex was tested at regular intervals to verify anesthesia depth. During surgical preparation, 0.2 ml–0.25 ml of the initial ketamine-xylazine solution was injected when needed to maintain deep anesthesia. The animals' core temperature was continuously monitored by a rectal probe and kept above 38°C (TC-1000 Temperature Controller, CWE Inc., Ardmore, USA). Tracheotomy was performed and an endotracheal tube was inserted. End-tidal CO_2 concentrations were monitored during the experiment.

#174557 - $15.00 USD Received 17 Aug 2012; revised 13 Nov 2012; accepted 23 Nov 2012; pub. 28 Nov 2012

Animal heads were secured in a customized rodent head holder that allowed adjustment along three axes. Preparation and recording from left and/or right ears of the animals were carried out sequentially. The animals' bullae were exposed by retroauricular incisions (Fig. 1(a)). Muscle tissue and soft tissue was dissected and the posterio-lateral part of the bulla was opened to access the round window niche without damaging the tympanic membrane. To access the round window, the bone of the bulla was carefully pierced with a hollow needle and partially removed using a micro rongeur to expose the middle ear and the basal turn of the cochlea, including the round window niche. Following the surgical preparation, xylazine concentration in the anesthetic solution was reduced to 5 mg/kg in order to prevent respiratory depression and bradycardia over the course of the experiments.

Hearing function was tested before and after surgery by recording a series of click-evoked auditory brainstem responses (ABRs) of increasing intensity (0–80 dB SPL). Middle-ear and cochlear function were considered normal for ABR thresholds below 40 dB SPL. All investigated animals satisfied this criterion. Subcutaneous Ag/AgCl electrodes were placed retroauricularly on both sides of the head for ABR recordings. Another Ag/AgCl electrode was subcutaneously inserted at the vertex of the skull at the interauricular line.

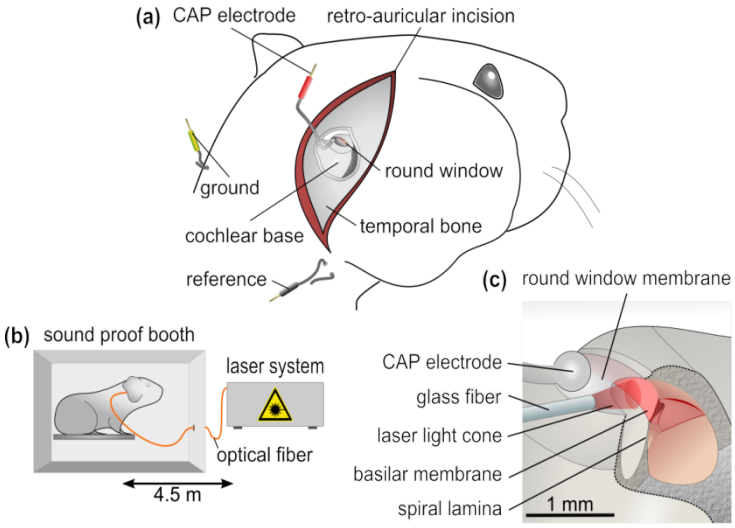

Fig. 1. (a) Schematic of the retroauricular access to the round window niche in the tympanic bulla. Electrode positions are shown relative to the surgical landmarks. (b) Experimental setup with soundproof booth, glass fiber, and laser system (objects not proportional). (c) A scaled section of the basal turn of the cochlea accessible through the round window. Emitted light from the tip of the glass fiber irradiates an area at the boundary between the bony spiral lamina and the basilar membrane. Nerve fibers innervating the hair cells in the organ of Corti traverse from the spiral lamina to the underside of the basilar membrane. The ball electrode for CAP recordings is located next to the glass fiber tip on the round window membrane.

In some cases a bone screw was placed at the same location and conductive contact to the dura mater was established using salt-free electrode gel (Spectra 360, Parker Laboratories Inc.). Condensation clicks of 50 µs duration were presented using a calibrated dynamic speaker (DT48 Beyerdynamic, Heilbronn, Germany) placed approximately 1 cm from the external meatus under free-field conditions. The recorded signals were filtered (Butterworth filter 6th order, high-pass frequency 200 Hz, low-pass frequency 5 kHz) and amplified by 100 dB using a filter and amplifier combination (F1 device, Otoconsult Company, Frankfurt (Main), Germany). One hundred recordings were made with a sampling rate of 100 kHz.

A small silver ball electrode (ø < 500 µm) with Teflon-insulated shaft was placed at the edge of the round window in close contact with the round window membrane (RWM) and with an impedance below 20 kΩ (Fig. 1(c)). The electrode wire was fixed to the temporal

#174557 - $15.00 USD Received 17 Aug 2012; revised 13 Nov 2012; accepted 23 Nov 2012; pub. 28 Nov 2012

bone (Histoacryl, B. Braun Melsungen AG, Germany) to ensure the position of the recording electrode remained stable throughout the experiment. Cochlear compound action potentials (CAPs) were recorded using the retroauricular Ag/AgCl electrode as reference. Acoustic CAPs were recorded using alternating 50 µs condensation and rarefaction clicks. The recorded signal was filtered (Butterworth filter 6th order, high-pass frequency 5 Hz, low-pass frequency 5 kHz) and amplified by 80 dB. The responses to 100 repetitions of each stimulus were averaged.

2.2. Laser stimulation

An optical parametric oscillator (OPO) employed as a tunable laser system was used for stimulation (Ekspla, NT342A, Vilnius, Lithuania). The pulse duration was 3–5 ns with a repetition rate of 10 Hz. The emitted laser light was coupled into a glass fiber (AFS105/125Y: 105 µm core, VIS-IR, Thorlabs, Newton, NJ, USA) to deliver the pulses into a soundproof room (Fig. 1(b)). The pulse energy was measured at the tip of the fiber (pyroelectric energy probe DPJ8, Spectrum Detector Inc., Oregon, USA). The OPO contained a variable attenuator and an additional reflective neutral density filter (ND10A, Thorlabs, Newton, NJ, USA). This allowed an adjustment of the attenuator's setting to obtain a constant energy at all wavelengths tested. A constant pulse energy of 6 µJ at the tip of the fiber was selected for the wavelength region of 420–2150 nm. The pulse energy distribution is Gaussian with a standard deviation of ≤0.4 µJ at a pulse energy of 6 µJ. The maximum pulse energy used in this study was 8 µJ, which corresponds to a maximum radiant exposure of 92 mJ/cm^2 at the fiber tip calculated with the nominal fiber core diameter. The glass fiber was cleaved before each experiment.

The optical fiber was carefully placed inside the tympanic bulla using a micromanipulator (MM33, Märzhäuser Wetzlar GmbH & Co. KG, Germany) and pointed towards the border between the basilar membrane and the bony spiral lamina, which is the position where both the hair cells and primary afferents of neurons could be irradiated by laser light. Stimulation was initially performed through the round window. In the first part of the experiment the fiber tip was not in contact with the RWM. When emitting laser pulses through the fiber, laser-evoked CAPs were measured according to the procedures described for acoustic CAPs, with the exception that the sampling rate was set to 500 kHz. From the start of the CAP recording and the laser pulse emission a delay of 840 µs was measured, using a silicon photo diode (S6468, Hamamatsu Photonics K. K., Hamamatsu City, Japan).

Subsequently, the RWM was carefully punctured using a fine cannula and the optical fiber was inserted directly into the cochlea (the target being the border of basilar membrane and spiral lamina) as before. With the punctured RWM, the recordings of laser-evoked CAPs were repeated in the same way as described above.

2.3. Deafening

Finally, to assess the function of the hair cells for the laser-generated CAP responses, the cochlea was deafened by intracochlear application 100 µl of 2.5% neomycin sulfate solution (Caesar & Lorentz GmbH, Hilden, Germany) and subsequent rinsing with Ringer's solution (Berlin-Chemie AG, Berlin, Germany). Subsequent recordings of CAP thresholds with condensation clicks at 100 dB SPL demonstrated profound hearing loss. Laser stimulation was repeated using the procedure described above.

3. Results

Following laser pulse stimulation, CAPs had a form that was well comparable with CAPs recorded using acoustic clicks (Fig. 2). Increasing SPL or increasing pulse energy resulted in an increase in peak-to-peak values of CAPs. The shape of both CAPs was similar, with the same characteristic minima and maxima (N1, P1, N2). For a further analysis, peak-to-peak values of the CAP (N1 to P1) were used and will subsequently be referred to as 'CAP

#174557 - $15.00 USD Received 17 Aug 2012; revised 13 Nov 2012; accepted 23 Nov 2012; pub. 28 Nov 2012

amplitude'. An artifact at 0.625 ms was observed during laser stimulation (marked by a triangle in Fig. 2), which was related to the switching impulse of the Pockels cell of the pump laser of the OPO. This artifact hence directly precedes the laser pulse emission.

To further quantify and compare the change of CAPs with increasing stimulus intensity, the CAP amplitude was plotted as a function of dB SPL and pulse energy (Fig. 3(a)), showing typical behavior for CAPs [14]. The same behavior was also observed for different wavelengths (Fig. 3(b)). However, the maximum CAP amplitude recorded was a function of the wavelength.

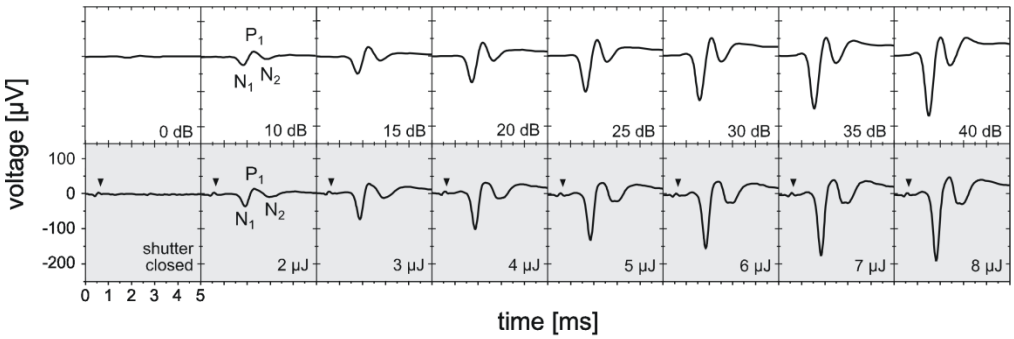

Fig. 2. Typical CAPs with acoustic click (top) and laser pulse stimulation (bottom, λ = 975 nm, 0–8 µJ; for 0 µJ the beam path was blocked, this being denoted as 'shutter closed'), as a function of sound level above threshold and pulse energy, respectively. The component at 0.625 ms (marked by a triangle) during laser stimulation (bottom) is an artifact due to the Pockels cell of the pump laser of the OPO. It indicates the time of laser pulse emission.

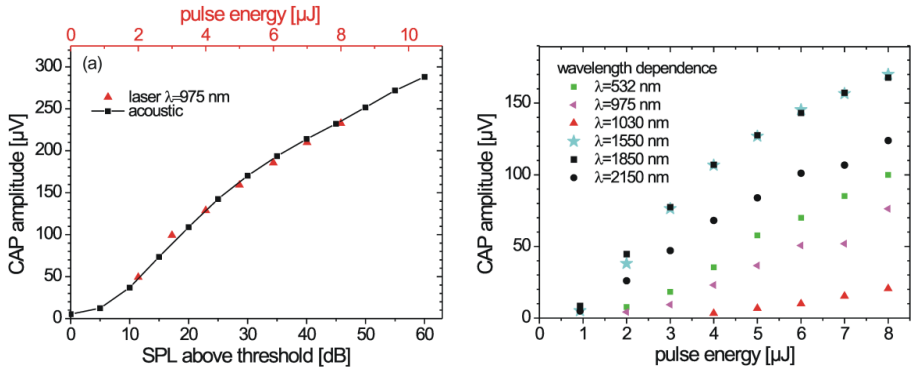

Fig. 3. (a) CAP amplitude as a function of SPL above threshold and pulse energy. The obtained sound pressure levels compare well with a previous study where sound was directly measured in air [9]. (b) CAP amplitude as a function of wavelength and pulse energy from another experiment (high-pass filter frequency 500 Hz instead of 5 Hz).

At constant pulse energy, the near-infrared wavelengths (1550 nm and 1850 nm) induced the largest CAP amplitudes. Therefore, the conversion of optical pulse energy into a cochlear response appears most efficient at these wavelengths. The wavelengths of 2150 nm, 532 nm, 975 nm, and 1030 nm followed with decreasing CAP amplitudes. When using 1850 nm wavelength, it was possible to achieve the same CAP amplitude using ≈60% less pulse energy than that used with 975 nm.

Subsequently, CAP amplitudes were compared during stimulation with 27 different wavelengths (Fig. 4(a)). The complex dependency of CAP amplitudes on wavelength contained several maxima (at ≈425 nm, ≈550 nm, ≈975 nm, ≈1370 nm) and minima (at ≈490 nm, ≈600 nm–845 nm, ≈1070 nm, ≈1440 nm, ≈1930 nm). For a comparison of 11 different cochleae and the inherent interindividual variability of maximal CAP amplitudes, it

#174557 - $15.00 USD Received 17 Aug 2012; revised 13 Nov 2012; accepted 23 Nov 2012; pub. 28 Nov 2012

was necessary to normalize the CAPs (Fig. 4(b)). The normalized data were well reproducible in different ears.

This complex relation is likely to result from the optical properties of the perilymph. The main component of perilymph is water. The larger amplitudes of laser-evoked CAPs at 1370 nm, 1550 nm, 1850 nm and 975 nm may thus arise because of the higher absorption coefficient of water at these wavelengths compared with that at 1070 nm and 845 nm [15,16]. However, at 532 nm the CAP amplitude should be even smaller since the water absorption coefficient is lower than at 845 nm. This was not the case. Consequently, additional chromophores must absorb the laser light at these wavelengths. Another possible candidate is hemoglobin [17]. Figure 4(c) shows CAP maxima (≈425 nm, ≈550 nm) and minima (≈490 nm, ≈600 nm–845 nm) related to the absorption coefficient μ of hemoglobin.

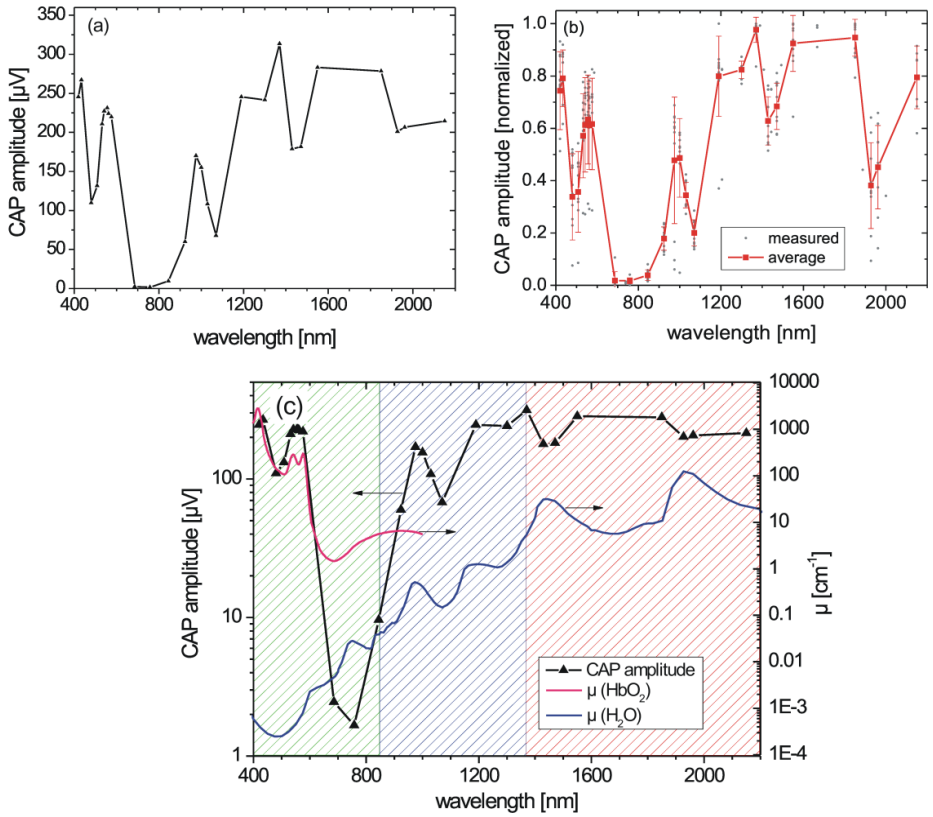

Fig. 4. (a) Representative CAP amplitude versus wavelength of the laser pulse in one cochlea. (b) Normalized CAP amplitudes versus wavelength for 11 cochleae. Standard deviation is depicted as error bar. (c) CAP amplitude of a typical individual shows analogy with the absorption coefficient of hemoglobin μ_{HbO2} for $\lambda \leq 845$ nm [17] and of water μ_{H2O} for $\lambda \geq 845$ nm [15,16]. For details on color coding, see Fig. 5 (green 420 nm $\leq \lambda \leq$ 845 nm; blue 845 nm $\leq \lambda \leq$ 1370 nm; red 1370 nm $\leq \lambda \leq$ 2150 nm).

To better quantify the results, normalized CAP amplitudes were correlated with absorption coefficients of hemoglobin [17] and water [15,16] for the given wavelengths. For each wavelength the absorption coefficient can be related to its corresponding CAP amplitude. A logarithmic correlation of the CAP amplitude and the hemoglobin absorption coefficient μ_{HbO2} was found for 420 nm $\leq \lambda \leq$845 nm (Fig. 5(a); $r^2 = 0.71$, $p<0.001$). For further details on all correlation functions, see Table 1.

#174557 - $15.00 USD Received 17 Aug 2012; revised 13 Nov 2012; accepted 23 Nov 2012; pub. 28 Nov 2012

Table 1. Details on correlation functions (for all correlation functions $p < 0.001$)

Figure	*a*	*b*	r^2	*n*	*Equation*
5(a)	–0.098 ± 0.035	0.275 ± 0.016	0.71	127	$Y = a + b \cdot \lg(x)$
CAP vs. μ_{H2O} for $\lambda < 845$ nm	–0.407 ± 0.083	–0.287 ± 0.027	0.48	126	$Y = a + b \cdot \lg(x)$
5(b) Section 1	0.670 ± 0.016	0.486 ± 0.022	0.85	92	$Y = a + b \cdot \lg(x)$
5(b) Section 2	1.367 ± 0.040	–0.462 ± 0.028	0.78	83	$Y = a + b \cdot \lg(x)$
μ_{HbO2} vs. μ_{H2O}	(0.558 ± 0.110) cm^{-1}	–0.785 ± 0.041	0.57	277	$Y = a \cdot x^b$ [18]
6(a) N1	(1.825 ± 0.034) ms	(–1.69 ± 0.20) µs/µV	0.84	15	$Y = a + b \cdot x$
6(a) P1	(2.354 ± 0.029) ms	(–1.87 ± 0.17) µs/µV	0.90	15	$Y = a + b \cdot x$
6(b)	(1.1689 ± 0.0048) ms	(–1.134 ± 0.025) µs/µV	0.985	33	$Y = a + b \cdot x$
7(b) top	(1.067 ± 0.017) ms	(–0.198 ± 0.025) ms	0.72	26	$Y = a + b \cdot x$
7(b) bottom	(1.142 ± 0.013) ms	(–0.360 ± 0.018) ms	0.94	26	$Y = a + b \cdot x$

Next, the CAP amplitudes were correlated with the absorption coefficient of water. A significant logarithmic negative correlation was observed for 10^{-4} $cm^{-1} \leq \mu_{H2O} < 0.004$ cm^{-1} ($r^2 = 0.48$, $p < 0.001$, see Table 1: CAP vs. $\mu_{H2O,}$ 420 nm $\leq \lambda \leq$845 nm, data not shown). However, the positive correlation of CAP amplitudes with the hemoglobin absorption coefficient had a larger correlation coefficient ($r^2 = 0.71$, $p < 0.001$) and the absorption coefficient for hemoglobin is greater than for water in these wavelengths, indicating that hemoglobin is the dominant absorber at wavelengths smaller than 845 nm (for details see annotation [18]). Wavelengths in this section are mostly in the visible range (420–845 nm, compare green hatching in Fig. 4(c).

For higher water absorption coefficients (0.004 $cm^{-1} \leq \mu_{H2O} \leq 5.5$ cm^{-1}), there was a positive logarithmic correlation ($r^2 = 0.85$, $p < 0.001$, blue hatching in Fig. 5(b)), denoting that with higher absorption coefficient a larger CAP amplitude is measured (wavelengths in this section are 924 nm, 1000 nm, 1070 nm, 1370 nm; compare blue hatching in Fig. 4(c)). For even higher water absorption coefficients (5.5 $cm^{-1} \leq \mu_{H2O}$) there was a negative logarithmic correlation ($r^2 = 0.78$, $p < 0.001$, red hatching in Fig. 5(b)), which resulted in the 'dips' in the CAP amplitude around 1440 nm and 1930 nm in Fig. 4.

In consequence, three different regions of correlation between the absorption coefficient and the CAP amplitude can be defined. These regions, in turn, correspond to three different wavelength regions (Figs. 5 and 4(c)), resulting in the complex dependency of CAP amplitude on wavelength:

- Positive correlation with μ_{HbO2} for 420 nm $\leq \lambda \leq$ 845 nm
- Positive correlation with μ_{H2O} for 845 nm $\leq \lambda \leq$ 1370 nm
- Negative correlation with μ_{H2O} for 1370 nm $\leq \lambda \leq$ 2150 nm

Another characteristic of the CAP response is the time of occurrence of the response peaks (their 'latency'). As mentioned above, the exact time of occurrence of the laser pulse was measured using a photo diode and the latency was determined with respect to this time (methods). In contrast to increasing CAP amplitude with increasing stimulus intensity, CAP latency (both for N1 and P1, see Fig. 2) decreases with increasing intensity [19]. This physiological behavior was observed for an acoustic stimulus (see Fig. 6(a)) as well as for the laser stimulus, even though the wavelength and pulse energy was varied (see Fig. 6(b)). There were linear correlations between the latency and the CAP amplitude for both stimulations (N1 $r^2 = 0.84$; $p<0.001$, P1 $r^2 = 0.90$, $p<0.001$, Fig. 6(b), $r^2 = 0.985$, $p<0.001$: see Table 1). This demonstrates that CAP amplitudes are the main factor determining CAP latencies. A relation of this kind would be unlikely if different stimulation mechanisms (e.g. direct neuronal stimulation and 'optical' stimulation via acoustic events) significantly contributed to the measured CAP, since each mechanism would most likely have a different latency. This also holds when all 27 wavelengths are included in the plot (Figs. 7(a) and 7(b)). For individual

#174557 - $15.00 USD Received 17 Aug 2012; revised 13 Nov 2012; accepted 23 Nov 2012; pub. 28 Nov 2012

animals, the correlation coefficient r^2 was between 0.52 and 0.94 (significant in all animals, $p<0.001$; the response latency was only determined in case of identifiable CAP with clear N1/P1 structure, cases where no such CAP could be identified where excluded from further analysis; compare 686 nm in Fig. 7(a)). Thus, neither laser pulse energy variation nor wavelength variation recruited a fundamentally different stimulation mechanism.

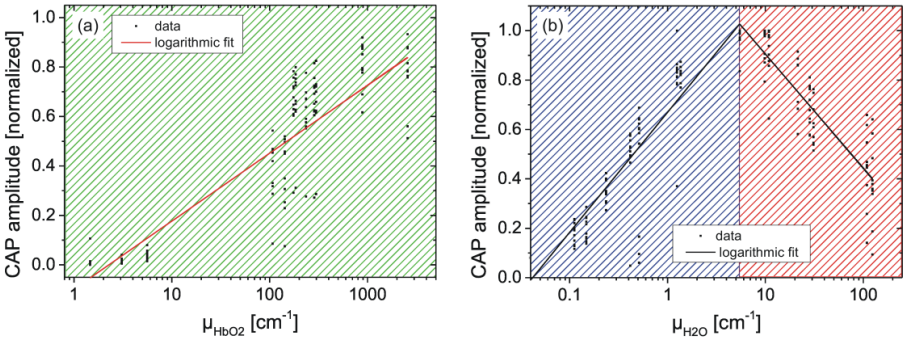

Fig. 5. (a) CAP amplitude versus hemoglobin absorption coefficient μ_{HbO2} (420 nm ≤ λ ≤ 845 nm). (b) CAP amplitude versus water absorption coefficient μ_{H2O} is divided into two sections: for 0.004 $cm^{-1} \leq \mu_{H2O} \leq 5.5$ cm^{-1} there is a positive correlation (blue hatching 845 nm ≤ λ ≤ 1370 nm) and for $\mu_{H2O} \geq 5.5$ cm^{-1} a negative correlation (red hatching 1370 nm ≤ λ ≤ 2150 nm).

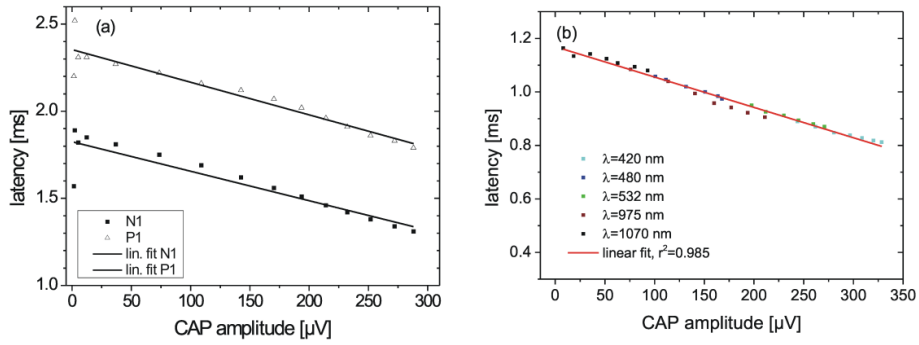

Fig. 6. Latency versus CAP amplitude ((a) acoustically evoked with varying SPL, (b) evoked by laser pulse stimulation with varying energy for wavelengths with high and low absorption coefficient for water and hemoglobin).

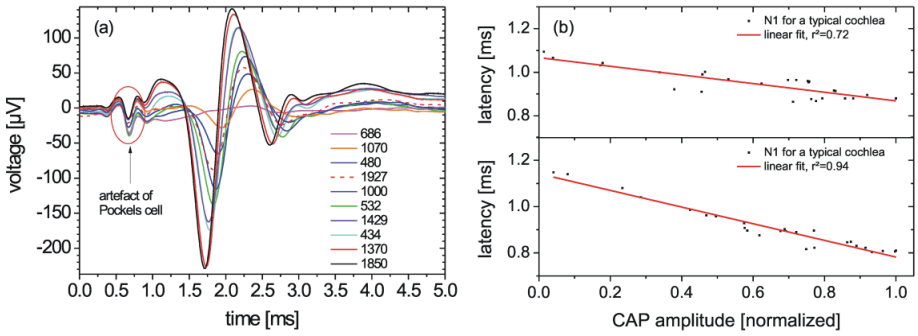

Fig. 7. (a) CAP responses for different wavelengths and constant pulse energy. CAPs show differences both in amplitudes and latencies of N1 and P1 depending on the wavelength. (b) N1 latency versus CAP amplitude evoked by laser pulse stimulation at different wavelength for a constant pulse energy for two typical individuals (top: same individual as in Fig. 6(a)), (bottom: individual with best correlation coefficient).

#174557 - $15.00 USD Received 17 Aug 2012; revised 13 Nov 2012; accepted 23 Nov 2012; pub. 28 Nov 2012

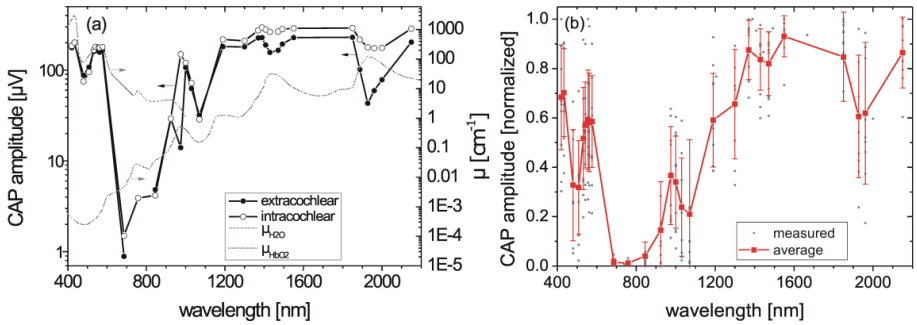

Fig. 8. (a) CAP amplitude for intra- and extracochlear stimulation in an individual animal as a function of wavelength. (b) Average of CAP amplitude for intracochlear stimulation of nine cochleae. Standard deviation is depicted as error bar.

Consequently, the CAP amplitude can be varied at constant pulse energy by changing the wavelength.

To investigate the effect of the fiber location with respect to the RWM, stimulation was performed outside and inside the cochlea (i.e. with intact and perforated RWMs). The CAP response for an intracochlear location of the fiber had characteristics similar to those obtained for an extracochlear location, also showing the correlation with hemoglobin and water absorption coefficient and the characteristic dips at ≈1440 nm and ≈1930 nm (shown in Fig. 8(a) for the same cochlea, the mean of all values for intracochlear stimulation Fig. 8(b)). Nonetheless, CAP amplitudes measured for intracochlear locations were not consistently larger than in cases without perforation, even though the distance to the modiolus was reduced during intracochlear stimulation.

After deafening of the ear, neither acoustic nor laser stimulation evoked a measureable CAP response (see Fig. 9) as already observed elsewhere [10]. To finally investigate the influence of the fiber tip position, e.g. distance to modiolus, a comparison of two positions was performed: The fiber tip was positioned pointing to the intact RWM and, representing an extreme case, pointing to the outer bone of the basal turn. Two wavelengths were used for both positions, one wavelength with a high absorption coefficient for water (Fig. 10(a), 1550 nm) and another with a high absorption coefficient for hemoglobin (Fig. 10(b), 420 nm). As a result, the position at the outer bone resulted in a smaller (but distinct) CAP amplitude than when the fiber tip position was pointing at the RWM (around 64% of the CAP amplitude at RWM at 1550 nm and 47% at 420 nm; see Fig. 10).

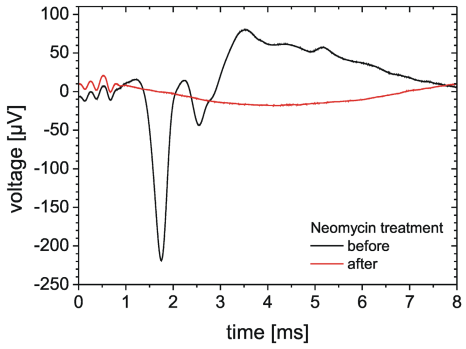

Fig. 9. CAP recordings of intra-cochlear stimulation before (black line) and after (red line) neomycin treatment (wavelength: 420 nm, pulse energy: 8 µJ).

#174557 - $15.00 USD Received 17 Aug 2012; revised 13 Nov 2012; accepted 23 Nov 2012; pub. 28 Nov 2012

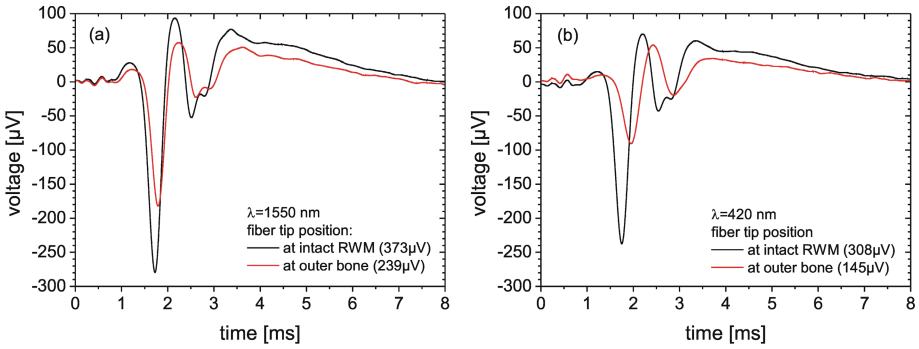

Fig. 10. Comparison of fiber tip position. CAP amplitude for the fiber tip pointing to the RWM (black line) is larger than when the tip is pointing to the outer bone of the basal turn (red line). Laser wavelengths are (a) 1550 nm and (b) 420 nm, representing wavelengths with high water and high hemoglobin absorption coefficients respectively.

4. Discussion

The present study demonstrates, for the first time, that laser pulse stimulation of the cochlea is related to water and hemoglobin as absorber materials. The complex relationship of CAP amplitudes and laser wavelengths was related to water and hemoglobin absorption, whereas three different regions could be identified: wavelengths where CAP amplitudes show a positive correlation with hemoglobin absorption coefficient, wavelengths where CAP amplitudes show a positive correlation with water absorption coefficient, and wavelengths where the CAP amplitudes showed a negative correlation with water absorption coefficient. Additional chromophores cannot be ruled out here. Melanin as a possible candidate, however, does not show characteristic features in the wavelength-dependent absorption coefficient in the way that hemoglobin and water do, so that it is not possible to exactly assess its contribution at present. The shape and latency of laser-evoked CAPs and those evoked by acoustic stimulation were comparable and behaved similarly with increasing intensity of stimulation. Also, their latencies were in linear relation to amplitudes in both modes of stimulation. Finally, the response disappeared after chemical deafening (see also [10]). Thus, absorption of laser pulses must generate an acoustic event picked up by functional hair cells.

4.1. Methodological discussion

The present experiments were limited to stimulation with nanosecond laser pulses. This is of importance, as these pulses result in the stress confinement condition for both water and hemoglobin [12,15–17]. It may be that stimulation at thermal confinement only results in a different outcome. Interestingly, stimulation at near-infrared wavelengths in thermal confinement was found to generate acoustic events that indicate similar optoacoustic phenomena as found in previous experiments [9]. Whether this holds for other wavelengths and other pulse durations remains to be tested.

In bone, absorption conditions and scattering are more complex. For wavelengths with a high water absorption coefficient (as in most experiments previously published), the greater part of the absorption takes place close to the fiber tip in the scala tympani or partly outside the cochlea. Consequently, the energy of the laser pulse reaching the bone (modiolus or spiral lamina) is most likely negligible.

The present experiments were confined to stimulation of the border of the basilar membrane and the spiral lamina. Depending on the penetration depth of laser light, this is the position where both the hair cells and primary afferents are located and can be irradiated. At other positions, the primary afferents enter the spiral lamina and pass underneath the bone. This was the reason why the stimulation site was selected. Nonetheless, the present experiments did not find any indication of a direct neuronal stimulation (compare [13]). We

#174557 - $15.00 USD Received 17 Aug 2012; revised 13 Nov 2012; accepted 23 Nov 2012; pub. 28 Nov 2012

cannot rule out that a different stimulation site results in a different outcome. One such suggested site is the soma of the spiral ganglion cells [20]. To allow stimulation at that site, wavelengths need to be selected which are absorbed neither in the scala nor in the bone so that they can penetrate into the Rosenthal's canal. Interestingly, in previous studies the majority of cochlear responses on 'deaf' animals were on ears with significant residual hearing (partially 40 or 60 dB SPL residual threshold [5,21]).

Finally, the distance between the glass fiber tip and the basilar membrane cannot be precisely controlled by the experimenter in the case of intracochlear stimulation. When the fiber is immersed in the scala tympani, the distance can be accurately assessed only by touching the basilar membrane or bone. That, however, would result in damage to the sensitive organ of Corti and contamination of the fiber tip with tissue. Variation in the exact position of the fiber within the scala tympani also explains the slightly higher variability in the outcome of intracochlear stimulation (compare standard deviation in Fig. 4(b) and Fig. 8(b)).

Of the phenomena that may be involved, plasma formation can be ruled out here. The critical free-electron density for inducing plasma formation with nanosecond pulses is 10^{20} cm^{-3} [12]. The corresponding radiant exposure threshold and threshold irradiance are ≈200 J · cm^{-2} and 3 · 10^{10} W · cm^{-2}, respectively [12]. Where penetration depth is 0.25 µm, the plasma formation threshold falls to 0.25 J · cm^{-2}. In our experiments the penetration depth remains above 3.9 µm and our maximum radiant exposure (0.092 J · cm^{-2}) is well below 0.25 J · cm^{-2} [12]. Additionally, our maximum irradiance is 3 · 10^7 W · cm^{-2}, i.e., three orders of magnitude below the irradiance threshold of 3 · 10^{10} W · cm^{-2}.

4.2. Discussion of the results

Although it has been well established that light and laser pulses generate sound [22,23], this has been demonstrated mainly for optoacoustic spectroscopy at much larger energies than those used in the present study [24]. However, our findings compare well with previous results on acoustic phenomena generated by laser light when interacting with water or humid air [9]. Our results point to other stimulation mechanisms than in [8]. Nevertheless, our pulse durations and energies were in the range used for stimulation of living tissue [5] and were three orders of magnitude lower than in [8]. The measured data suggest an acoustic laser-generated phenomenon activating the cochlea (compare also [9]) that disappears after deafening (compare [10]). Interestingly, these results are not in discrepancy with the mechanisms demonstrated on the lipid bilayer [8]: pressure rise as the consequence of the optoacoustic phenomenon is another possible explanation of the bilayer experiment. We propose a stress confinement-related process with compression-relaxation waves in air and tissue that is detectable by the cochlea. Interestingly, even if laser light was directed at the outer bone at the basal turn of the cochlea, a CAP of ≈60% amplitude was recorded in the present study. This experiment clearly demonstrates that nanosecond laser pulse stimulation of a normal-hearing ear results in predominantly acoustic activation. Other potential phenomena such as direct neuronal stimulation might be prevented by scattering and absorption of laser light in the bone. Measured responses on acoustic or laser-evoked stimulus disappeared after deafening. This laser stimulation therefore depends on functional hair cells. Similar results were obtained with other stimulation paradigms [25]. However, numerous differences in methodology preclude direct comparison. At the chosen stimulation site in the present study, cochlear responses were dependent on absorption but not directly on wavelength.

Finally, it has been well established that peripheral nerves and myocardial cells can respond to laser pulses [26–28]. In our laboratories, too, we observed facial nerve stimulation (data not shown). These may result from pressure waves and mechanoelectrical excitation described on axons of neurons [29,30]. Consequently, one possible mechanism of cochlear stimulation could result from a direct pressure effect on the basilar membrane by the laser pulse, particularly in the present experiments where the stimulation was aimed at the basilar

#174557 - $15.00 USD Received 17 Aug 2012; revised 13 Nov 2012; accepted 23 Nov 2012; pub. 28 Nov 2012

membrane. An uplifting of the basilar membrane in consequence of the pressure pulse would activate the hair cells, too (compare with [11]). Whether this may be a mechanism that is distinct from acoustic ('audible') phenomena generated in the cochlear fluid remains to be investigated. Wherever the transformation from light to pressure appears, the mechanism is optoacoustic in nature. A direct absorption at the basilar membrane or bone is possible at wavelengths with low absorption in the perilymph [10,11]. Nonetheless, more experiments are required to elucidate these phenomena in detail.

The fact that laser-induced CAP amplitude-latency relations were independent of wavelength and showed a linear relation without discontinuities, indicates that the present results were not due to two or more different stimulation mechanisms, such as optoacoustic and direct neuronal stimulation. In the present experiments, laser-evoked CAPs had a shorter latency compared with acoustic stimulation (compare Figs. 6(a) and 6(b)). The difference can be explained by the frequency-dependent delays (that are in the ms range) in excitation evoked by the travelling wave in the cochlea in response to click stimulation, compared with the detection site of the laser stimulation at the high-frequency part of the cochlea [31]. Additionally, acoustic signals are subject to delays owing to the propagation distance of the speaker to the tympanic membrane and the middle ear [32]. However, laser-evoked CAPs had a longer latency than typical responses to electrical stimulation of the auditory nerve [33].

One finding remains puzzling: the negative correlation of the CAP amplitude with water absorption coefficients greater than 5.5 cm^{-1}, most prominently expressed in the notches of CAP amplitudes for wavelengths of 1430 and 1930 nm. This has been reported earlier, whereas the interpretation is in disagreement with our experimental observation [34]. At present, we have not enough evidence to provide the eventual explanation for this phenomenon. However, there are several hypothetical possibilities that can be discussed:

1. A temperature rise of 48 K shifts the maximum of water absorption coefficient from 1930 to 1915 nm [35]. The temperature increase at 1927 nm can be estimated to be below 2 K per pulse. The thermal relaxation time at that wavelength is $\tau = 46$ ms, consequently no accumulation of temperature is expected at a repetitive stimulation of 10 Hz. However, the negative correlation cannot be explained by this hypothesis.

2. A possible shielding effect of water vapor or humid air [9] was ruled out since a CO_2 and dry-air purge into the middle ear during the measurement was without effect (data not shown). Stimulation inside of the cochlea also resulted in a similar effect, arguing against this possibility.

3. At wavelengths with a higher absorption coefficient, both the penetration depth (d) and the absorption volume (V) are smaller (see Table 2). For low absorption coefficients a cone-like acoustic source is formed along the beam (Fig. 11(a), compare with measurements in [9]). For higher absorption coefficients the pulse might be absorbed in a smaller volume (Fig. 11(b)) and vapor bubbles might be generated (compare [12,36]). They scale in size and life time depending on the absorption coefficient [12,36]. If their lifetime would exceed 100 ms, the temporal pulse-to-pulse distance in our setup, the vapor bubble might be in the beam path disturbing the pulse delivery and a negative correlation could be explained. However, so far we did not investigate the bubble dynamics. Further investigation with schlieren photography will bring insight into this effect [36].

Table 2. Absorption coefficient and related absorption volume

λ /nm	*1070*	*1370*	*1850*	*1927*
d/mm	67.55	1.83	1.02	0.08
μ/cm^{-1} [15,16]	0.148	5.45	9.85	124
$V/10^{-13}m^3$	$9.2 \cdot 10^7$	2910	681	8.9

#174557 - $15.00 USD Received 17 Aug 2012; revised 13 Nov 2012; accepted 23 Nov 2012; pub. 28 Nov 2012

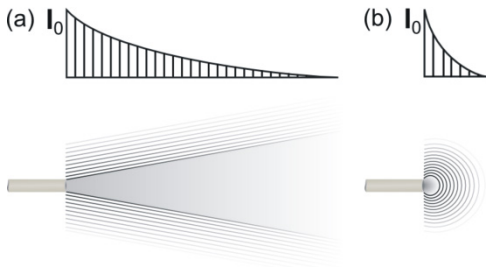

Fig. 11. Schematic of different shape of absorption volume and possible shape of pressure sources for (a) $\mu < 5.5\ cm^{-1}$ and $V >> 1$ and (b) $\mu > 5.5\ cm^{-1}$ and $V << 1$.

In total, the present experiments demonstrate that pulsed laser stimulation-evoked CAP amplitudes are strongly dependent on water and hemoglobin absorption.

5. Conclusion

Nanosecond laser pulses applied to the cochlea resulted mainly in optoacoustic events in a wide range of wavelengths (420–2150 nm). These events result from absorption of energy by water and hemoglobin, depending only indirectly on wavelength. Absorption in wavelengths between 420 and 845 nm is dominated by hemoglobin; longer wavelengths are absorbed by water. The present experiments also show that complete deafening of the ear (owing to pharmacologically induced hair cell damage) results in loss of responsiveness to nanosecond laser pulses. Consequently, laser-evoked cochlear responses depend on the integrity of hair cells. This points to hair cells as the main detector for laser-irradiation related acoustic events with nanosecond laser pulses.

Acknowledgments

This work was partially funded by the German Research Foundation (DFG) within the special research area SFB Transregio 37. We thank Eddy and Daniela Kühne for their support, and Diego Sabucedo Vilaboa for some of the data analysis.

#174557 - $15.00 USD Received 17 Aug 2012; revised 13 Nov 2012; accepted 23 Nov 2012; pub. 28 Nov 2012